

# In doping and post-treatment effect on holographic properties in In:Ce:Cu:LiNbO<sub>3</sub> crystal

TAO ZHANG<sup>a\*</sup>, TAO GENG<sup>a</sup>, YAN-TANG DONG<sup>a</sup>, QIANG DAI<sup>a</sup>, WEI-MIN SUN<sup>a</sup>, YU-HENG XU<sup>b</sup>

<sup>a</sup>College of Science, Harbin Engineering University, Harbin 150001, China

<sup>b</sup>School of Astronautics, Harbin Institute of Technology, Harbin 150001, China

A series of triply-doped In:Ce:Cu:LiNbO<sub>3</sub> crystals with a varying level of In doping were grown by Czochraski technique in air atmosphere, and some samples were made post-treatment such as oxidation and reduction in different powders at high temperature. The two-wave coupling experiment was employed to measure the holographic properties such as diffraction efficiency, erasure time, the relation between light intensity and photoconductivity, optical excited carrier style, and loss signal-to-noise-ratio coefficient. The results indicate that the holographic properties can be improved by proper level of In doping and post-treatment in In:Ce:Cu:LiNbO<sub>3</sub>. The underlying mechanism on the effect of In doping and post-treatment on the properties is also discussed in terms of the ion location in the host lattice and photoconductivity change in LiNbO<sub>3</sub>.

(Received February 8, 2008; accepted June 30, 2008)

**Keywords:** LiNbO<sub>3</sub> crystals, In doping, Post-treatment, Holographic properties

## 1. Introduction

LiNbO<sub>3</sub> crystal is a kind of multifunctional material for its extensive industrial applications in the field of piezoelectricity [1], acoustic-optics [2], linear [3] and nonlinear optics [4] etc. Congruent LiNbO<sub>3</sub> crystal generally has good optical quality and mass productivity. However, the pure congruent crystal has little practical application served as a holographic storage medium due to its two kinds of serious disadvantages. One is the poor photorefractive effect such as long response time, low diffractive efficiency, low sensitivity and strong light-scattering etc; the other is data volatility in the readout process of holograms.

So far, there are many methods available for improving the photorefractive properties. Doping various rare earth (like Ce [5], Tb [6] etc.) and transition metal (like Fe [7], Mn [8], Cu [9] etc.) ions can increase the photorefractive effect such as larger diffractive efficiency, higher sensitivity and bigger dynamic range. Among them, Fe-doped LiNbO<sub>3</sub> crystal is widely investigated and considered as one of the most promising material applied in holographic memory. On the other hand, the doping ion also brings insensitive laser-induced scattering and low signal-to-noise-ratio. In 1980, Zhong et al. [10] first reported that LiNbO<sub>3</sub> doped with 4.6 mol% MgO had the ability to resist light intensity about 100 times greater than pure LiNbO<sub>3</sub>. Later, other optical damage resistance impurities, Zn [11] and Sc [12], have been found subsequently. Indium reported by Volk and Rubinina [13] is a new kind of impurity similar to Mg and Zn, and can strengthen the optical damage resistance ability in LiNbO<sub>3</sub> crystal. Moreover, the post-treatment (reduction or oxidation) has demonstrated to be an effective means that it can polish up the photorefractive properties by virtue of changing the valence state of rare earth and transition metal ion in the crystal [14]. Finally, the control of the Li/Nb ratio in LiNbO<sub>3</sub> crystal is also of key importance for

this performance of crystal [15]. But the non-congruent composition actually add the difficulty in growing high quality crystal with compositional-inhomogeneity-free. For solving the problem on data volatility, in 1998, Buse et al. [16] presented the realization of nonvolatile two-color holographic storage without perplexing thermal or electrical fixing in Fe:Mn:LiNbO<sub>3</sub> crystals. Afterward, Liu et al. [17, 18] found that Ce:Cu:LiNbO<sub>3</sub> was a more useful photorefractive crystal than Fe:Mn:LiNbO<sub>3</sub> in nonvolatile holographic recordings. Taking into account of the roles of Ce-Cu co-doping, In doping and post-treatment, it is desirable to obtain good photorefractive effect and nonvolatile holographic storage in Ce:Cu:LiNbO<sub>3</sub> crystal through In doping and post-treatment.

In this work, we chose oxide In<sub>2</sub>O<sub>3</sub>, CeO<sub>2</sub> and CuO as doping impurities for improving the entire holographic properties to grow triply-doped In:Ce:Cu:LiNbO<sub>3</sub> single crystals by conventional Czochralski method, and studied systematically the influence of indium and post-treatment on optical properties. Also, the underlying mechanisms are discussed by the ion location in the host lattice and photoconductivity change in LiNbO<sub>3</sub>.

## 2. Experimental Details

### 2.1 Crystal growth and sample preparation

Several triply-doped In:Ce:Cu:LiNbO<sub>3</sub> crystals were grown from congruent melts of Li/Nb=0.946 (mole ratio) using Czochralski method in air atmosphere. The used raw materials are Li<sub>2</sub>CO<sub>3</sub>, Nb<sub>2</sub>O<sub>5</sub>, In<sub>2</sub>O<sub>3</sub>, CeO<sub>2</sub> and CuO with spectroscopical purity. The starting compositions are summarized in Table 1. Following precisely weighed and thoroughly mixed for 12 h, respectively, the raw materials were fully calcined at 700 °C for 2 h and then sintered at 1150 °C for 2 h so as to form polycrystalline bulk. Growth runs were carried out under the optimum technology conditions: temperature gradient of 40~50 °C /cm along

the furnace axial direction, rotating rate of 15~25 rpm, and pulling rate of about 2 mm/h. The typical as-grown crystal sizes were about 30 mm in diameter and 30 mm in length. Since as-grown  $\text{LiNbO}_3$  crystals are one-dimensional ferroelectrics and exists spontaneous polarizing. Thus, they are required to form single domain structure from multi-domain structure by polarizing treatment for holographic storage. In the experiment, the crystals were placed in a furnace where the temperature gradient was 5  $^{\circ}\text{C}/\text{cm}$  for polarizing with 5  $\text{mA}/\text{cm}^2$  dc currents for 30

min at 1200  $^{\circ}\text{C}$ . For optical characterization, a number of (010)-plane slices were cut from the middle of the crystals, and then polished to optical grade smoothness using SiC powder and 0.25  $\mu\text{m}$  diamond solution. Post-treatment was fulfilled by embedding some wafers into  $\text{Li}_2\text{CO}_3$  powder to be reduced at 550  $^{\circ}\text{C}$  for 6, and embedding some wafers into  $\text{Nb}_2\text{O}_5$  powder to be oxidized at 1150  $^{\circ}\text{C}$  for 10 h, respectively. Likewise, they were polished (see table 1).

Table 1. Summary of doping level, sample size, and post-treatment for the crystals.

| Samples | [ $\text{In}_2\text{O}_3$ ]<br>(mol%) | [ $\text{CeO}_2$ ]<br>(mol%) | [ $\text{CuO}$ ]<br>(wt%) | Crystal size<br>( $\text{mm}^3$ ) | Wafer size<br>( $\text{mm}^3$ ) | Post-treatment |
|---------|---------------------------------------|------------------------------|---------------------------|-----------------------------------|---------------------------------|----------------|
| I-A     | 0.5                                   | 0.2                          | 0.015                     | $\Phi 30 \times 26$               | $10 \times 3 \times 15$         | as-grown       |
| I-O     |                                       |                              |                           |                                   |                                 | oxidation      |
| I-R     |                                       |                              |                           |                                   |                                 | reduction      |
| II-A    | 1                                     | 0.2                          | 0.015                     | $\Phi 30 \times 28$               | $10 \times 3 \times 15$         | as-grown       |
| II-O    |                                       |                              |                           |                                   |                                 | oxidation      |
| II-R    |                                       |                              |                           |                                   |                                 | reduction      |
| III-A   | 1.5                                   | 0.2                          | 0.015                     | $\Phi 30 \times 30$               | $10 \times 3 \times 15$         | as-grown       |
| III-O   |                                       |                              |                           |                                   |                                 | oxidation      |
| III-R   |                                       |                              |                           |                                   |                                 | reduction      |

## 2.2 Experimental equipment and measurement

Holographic measurement was carried out with a two-wave coupling experiment in the transmission geometry. A schematic diagram of the experimental setup is shown in Fig. 1. A frequency-doubled Nd:YAG laser ( $\lambda = 532 \text{ nm}$ ) was split into two mutually coherent and extraordinarily polarized beams, which were made to intersect symmetrically inside the crystal with the crossing angle of 20° in air. The grating vector of written holograms was always aligned along the crystal's  $c$  axis to utilize the largest electro-optic coefficient  $\gamma_{33}$ . The intensity ratio between the two beams (labeled as signal beam  $I_R$  and reference beam  $I_S$ , respectively) was adjusted by rotation of half-wave plate HW1 to be equal (100  $\text{mW}/\text{cm}^2$ ).

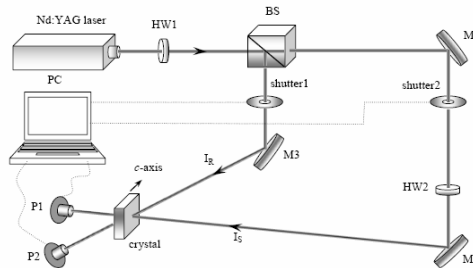


Fig. 1. Light path scheme of two-wave coupling experiment.  $M_1, M_2, M_3$ : mirrors;  $HW1, HW2$ : half-wave plate;  $BS$ : beam splitter;  $P1, P2$ : photo-detectors;  $I_R$ : reference beam;  $I_S$ : signal beam.

## 3. Experimental results and discussion

### 3.1 Diffraction efficiency and erasure time

While writing gratings, signal beam was blocked by a shutter from time to time to measure the holographic

diffraction efficiency  $\eta$ . Here  $\eta$  was defined as  $I_d/(I_d+I_t)$ , where  $I_d$  and  $I_t$  were the diffracted and transmitted intensities of the readout beam, respectively. A few percent of diffraction efficient could be achieved. During the grating building up,  $\eta$  increased by exponential law with time. After the grating reached the saturation, the signal beam was blocked, and the written grating could be erased by illumination with the reference beam. In contrast to the recording, the erasure process shows exponential decay. Fig. 2 illustrates the evolution of  $\eta$  during recording and erasing in  $\text{Ce:Cu:LiNbO}_3$ . At the same time, the corresponding saturated refractive index change  $\Delta n_{sat}$  can be calculated by Kogelnik's formula as [19]

$$\eta_{max} = \sin^2\left(\frac{\pi d \Delta n_{sat}}{\lambda \cos \theta_{cry}}\right), \quad (1)$$

where  $d$  is the thickness of the wafer,  $\lambda$  is the wavelength of laser, and  $\theta_{cry}$  is the internal half angle between the two incident laser beams. The experimental results are given in table 2.

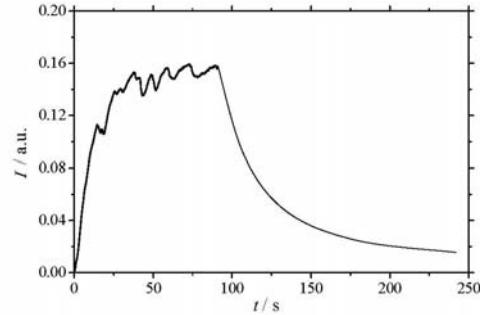


Fig. 2. Curve of diffraction efficiency dependence on time as grating building up and erasure.

Table 2. Holographic properties of the crystals.

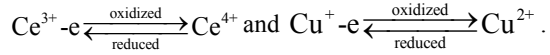
| Samples | Maximum          | Response time | Erasure time | Saturation            | Loss of signal-to-noise ratio |
|---------|------------------|---------------|--------------|-----------------------|-------------------------------|
|         | $\eta_{max}$ (%) | $\tau_r$ (s)  | $\tau_e$ (s) | $\Delta n_{sat}$      | LSNR                          |
| I-A     | 55.0             | 502           | 850          | $5.53 \times 10^{-5}$ | 9.8                           |
| II-A    | 42.6             | 253           | 466          | $4.70 \times 10^{-5}$ | 4.7                           |
| III-A   | 37.3             | 147           | 320          | $4.34 \times 10^{-5}$ | 2.5                           |
| III-O   | 39.7             | 456           | 872          | $4.51 \times 10^{-5}$ | 1.3                           |
| III-R   | 18.1             | 18            | 31           | $2.90 \times 10^{-5}$ | 5.6                           |

From table 2, it can be observed that with the increasing of In doping content, the diffraction efficiency decreases and the response time becomes short as well. Under the same In doping content, the reduced crystal exhibits the fastest respond time and the oxidized crystal has the highest diffraction efficiency.

It is well known that the photoconductivity is directly proportional to the donor center concentration and is inversely proportional to the acceptor center concentration. The saturated refractive index change is proportional to the photovoltaic field, which can be described by relation

$$E_{ph} = j_{ph} / \sigma \propto [\text{acceptor}], \quad (2)$$

where  $j_{ph}$  is photovoltaic current and  $\sigma$  is conductivity. In In:Ce:Cu:LiNbO<sub>3</sub> crystals, the following reactions serve to describe the post-treatment process:



In the reactions, Ce<sup>3+</sup> and Cu<sup>+</sup> are the donor centers, Ce<sup>4+</sup> and Cu<sup>2+</sup> are the acceptor centers. During post-treatment oxidation processing, the donor centers will decrease and the acceptor centers will increase by contrast. Thus, it results in the drop of photoconductivity and the improvement of saturated refractive index. Therefore, the decreased photoconductivity lengthens the erasure time, and the increased refractive index enhances the diffraction efficiency. In the case of reduction treatment, the reverse results can be obtained.

When In is doped in LiNbO<sub>3</sub> crystal, it will increase the photoconductivity a little. So the erasure time will be shortened with the increase of In doping concentration. On the other hand, the In doping will also change the capture section of carriers in crystal. Especially, the higher In doping concentration, the more the capture section of carriers will decrease. Consequently, this makes the space-charge field fall as well as the diffraction efficiency.

### 3.2 Light intensity dependence of photoconductivity

Under the illumination of uniform laser, the written gratings in the crystal will decay up to being completely erased. By solving Kukhtarev equations, the space-charge field with time can be derived as [20]

$$E_{sc}(t) = E_{sc}(0) e^{-t/\tau_{sc}}, \quad (3)$$

where  $\tau_{sc}$  is the erasure time constant, which has very close relation with the conductivity by

$$\tau_{sc} = \frac{\epsilon \epsilon_0}{\sigma_d + \sigma_{ph}}, \quad (4)$$

where  $\epsilon$  is the relative dielectric constant and  $\epsilon_0$  is the dielectric constant of vacuum,  $\sigma_d$  and  $\sigma_{ph}$  are photoconductivity and dark conductivity, respectively. Since holographic grating strength in our crystals show no clear loss in the darkness with a rather long time,  $\sigma_d$  in equation (4) can be neglected in the measurement range of light intensity, i.e.  $1/\tau_{sc} \propto \sigma_{ph}$ . Accordingly, the light intensity dependence of the photoconductivity can be determined by measuring the erasure time constant at different light intensities. It has been demonstrated that when there exists only one energy level to participate the photorefractive process, the photoconductivity is a linear function of light intensity. On the other hand, when there are two or more energy levels to concern the process, the relation between them is nonlinear. Figures 3-4 show the experimental results.

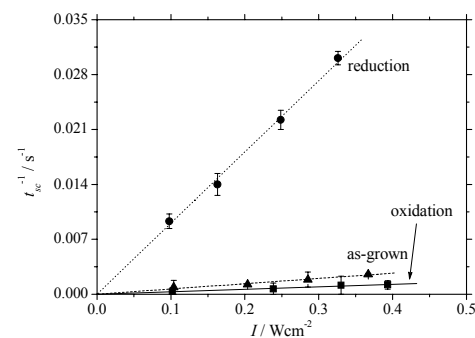


Fig. 3. Dependence of light intensity on erasure time in In(3mol%):Ce:Cu:LiNbO<sub>3</sub> crystal at the different state of post-treatment.

As shown in Fig. 3, although the In (3 mol%):Ce:Cu:LiNbO<sub>3</sub> crystal has two energy levels, the light intensity is still proportional to photoconductivity. This indicates that the photorefractive process is only

related to one energy level in the three states of In:Ce:Cu:LiNbO<sub>3</sub> crystals. In addition, the photoconductivity in the crystals is different for the equal light intensity under the different post-treatment. Among them, the photoconductivity of the reduced is the biggest, that of the as grown bigger and that of the oxidized the smallest. It has been known that the photoconductivity is directly proportional to the free electron concentration in crystal. In the reduced crystal, the donor concentration is higher and therefore the free electron concentration is also higher, thus it results in the bigger photoconductivity and the shorter response time (see table 2). From figure 4, one sees that the photoconductivity increases with the increase of In doping concentration at the equal light intensity. It is concluded that the faster response time can be obtained by high content of In doping in LiNbO<sub>3</sub> crystal.

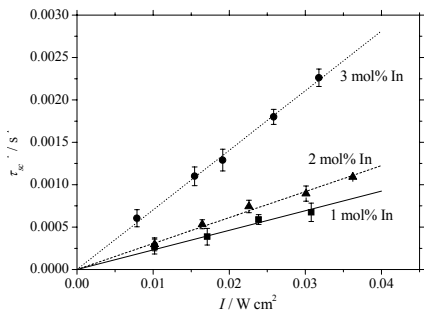


Fig. 4. Dependence of light intensity on erasure time in In:Ce:Cu:LiNbO<sub>3</sub> crystal with a varying level of In doping.

### 3.3 Optical excited carrier style

The setup in Fig. 1 was used in the experiment. During the erasure of the written gratings, the beam used to erase gratings will interfere with its diffraction beam in crystals and new gratings will be written in. The interaction between the new and the old gratings influences the erasure rate of the gratings<sup>[21]</sup>. Under the geometry as figure 1, when the electron is the dominant optical excited carrier in crystals, the erasure rate of the gratings with the signal beam  $I_S$  illuminating is faster than that with the reference beam  $I_R$ , and it is reverse when the vacancy is the dominant optical excited carrier.

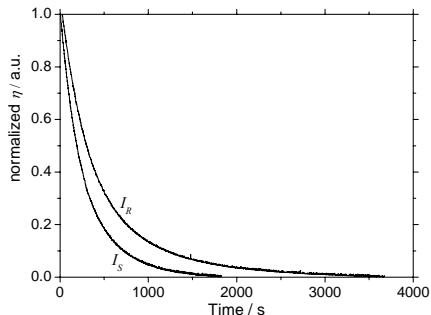


Fig. 5. Erasure curves of as-grown In(3 mol%):Ce:Cu:LiNbO<sub>3</sub> crystal.

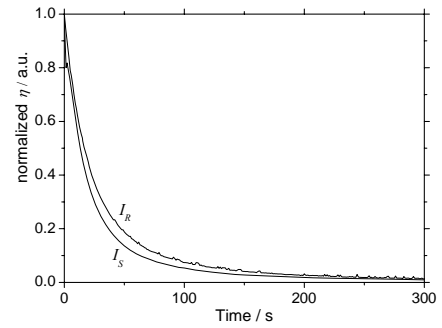


Fig. 6. Erasure curves of reduced In(3 mol%):Ce:Cu:LiNbO<sub>3</sub> crystal.

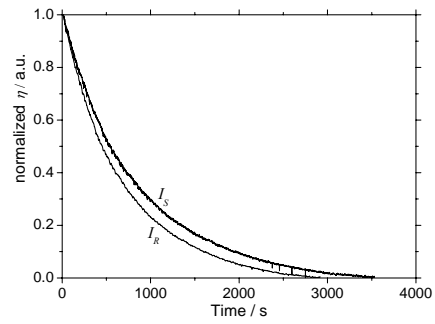


Fig. 7. Erasure curves of oxidized In(3 mol%):Ce:Cu:LiNbO<sub>3</sub> crystal.

The decay curves of the photorefractive gratings erased with  $I_R$  and  $I_S$  are shown in figures 5 to 9. From figures 5 to 7, it can be seen that the erasure speed by signal beam is faster than by reference beam for the In(3 mol%):Ce:Cu:LiNbO<sub>3</sub> crystal at the as-grown and reduced state. So it is suggested that the electron is the main style of the optical excited carrier in the erasure process. But at the oxidized state of this crystal, the erasure speed by reference beam is faster than by signal beam, and this indicates the vacancy is the dominant optical excited carrier. Moreover, in the three as-grown Ce:Cu:LiNbO<sub>3</sub> crystals doped with varied In content, the erasure speed by signal beam is always faster than by reference beam, and therefore the electron dominates the optical excited carrier (see figures 5, 8 and 9).

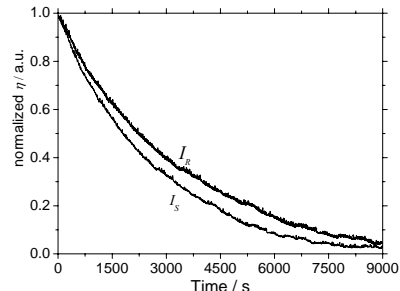


Fig. 8. Erasure curves of as-grown In(2 mol%):Ce:Cu:LiNbO<sub>3</sub> crystal.

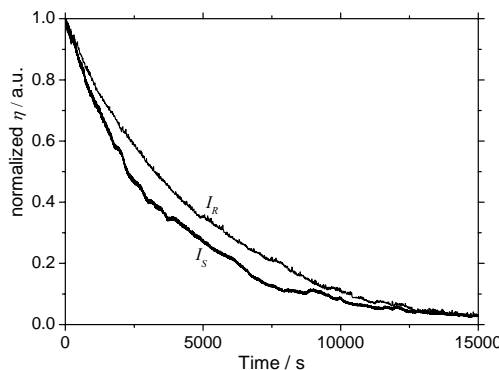


Fig. 9. Erasure curves of as-grown In(1mol%):Ce:Cu:LiNbO<sub>3</sub> crystal.

### 3.4 Loss signal-to-noise-ratio coefficient

For holographic storage materials, low scattering will result in strong photo-damage resistance ability and high signal-to-noise ratio (*SNR*). Thus the loss signal-to-noise-ratio coefficient (*LSNR*) is also introduced to evaluate quantitatively the destroying degree of the reconstructed image, which is defined as [22, 23]

$$LSNR = 10 \times \log(SNR_0 / SNR_1), \quad (5)$$

where *SNR*<sub>0</sub> and *SNR*<sub>1</sub> are the signal-to-noise-ratio of original transmitting image and retrieved image after the noise grating has been built in the same crystal, respectively. Here *SNR* is believed to be objective evaluating the reconstructed image quality and expressed as

$$SNR = \frac{I_1 - I_0}{\sigma_1 + \sigma_0}, \quad (6)$$

where  $\sigma_1$  and  $I_1$  ( $\sigma_0$  and  $I_0$ ) are the square difference of and intensity of bright unit (dark unit) in the image [24]. The *LSNR* values are also given in table 2. It is clearly observed that *LSNR* decreases with the increase of In doping content. How does In doping affect the photo-damage resistance ability in In:Ce:Cu:LiNbO<sub>3</sub> crystals? When the doping concentration of In is below its threshold, In ions replace the anti-site Nb<sub>Li</sub><sup>4+</sup> preferentially, and other two kinds of Ce, Cu ions occupy Li sites under lower In doping concentration. At this time, the capture section of the electron acceptors with Ce<sup>4+</sup> and Cu<sup>2+</sup> does not significantly change. The increasing photoconductivity, which is mainly attributed to the decrease of anti-site Nb<sub>Li</sub>, induces the decrease in *LSNR*. As the In doping concentration increases up to the threshold, Nb<sub>Li</sub><sup>4+</sup> is completely canceled and part of In ions start to substitute Nb sites. Simultaneously, Ce and Cu ions on the Li sites will be repelled to the Nb sites by In ions, so Ce<sub>Nb</sub><sup>+</sup> and Cu<sub>Nb</sub><sup>3-</sup> form, which reduce the capture section and enhance the photoconductivity since Ce<sub>Nb</sub><sup>+</sup> and Cu<sub>Nb</sub><sup>3-</sup> have a lower ability to trap electrons than Ce<sub>Li</sub><sup>3+</sup> and Cu<sub>Li</sub><sup>+</sup> do.

So, sample III-A has the least *LSNR* in three as-grown crystals. On the other hand, oxidation treatment also decreases the *LSNR*; by contrast, reduction treatment increases the *LSNR*. It is assumed that it is Ce<sup>3+</sup> and Cu<sup>+</sup> that induce scattering noise in LiNbO<sub>3</sub> crystal, and they are probably the centers of scattering noise when the crystal is irradiated by strong signal light. Comparing the post-treatment (samples: III-A, III-O and III-R), it is concluded that oxidation treatment can suppress the noise in readout effectively.

### 4. Conclusions

In conclusion, a series of triply-doped In:Ce:Cu:LiNbO<sub>3</sub> crystals with a varying level of In doping were grown by Czochraski technique, and some samples were made post-treatment such as oxidation and reduction. Based on two-wave coupling experiment, it is found that In doping and post-treatment are of key importance for improvement of the holographic properties in In:Ce:Cu:LiNbO<sub>3</sub> crystals. Analysis shows that the increased photoconductivity is mainly responsible for the excellent photorefractive comprehensive properties. It is believed that In:Ce:Cu:LiNbO<sub>3</sub> crystal is a promising holographic storage medium.

### Acknowledgements

This work was supported by a grant from the research fund of Harbin Engineering University (HEUFT06032), the science-technology creative foundation for young scientists of Harbin City (2007RFQXG031), and the specialized research fund for the doctoral program of higher education institutions of China (20070217013).

### References

- [1] M. Tasson, H. Legal, J. C. Gay, J. C. Peuzin, F. C. Lissalde, *Ferroelectrics* **13**(1), 479 (1976).
- [2] A. Lawrow, C. N. Pannell, M. Negoita, P. St. J. Russell, J. Webjörn, *Opt. Commun.* **144**, 161 (1997).
- [3] B. Wacogne, J. P. Goedgebuer, H. Porte, *Opt. Lett.* **19**, 1334 (1994).
- [4] Y. Chen, W. Yan, D. Wang, S. Chen, G. Zhang, J. Zhu, Z. Wei, *Appl. Phys. Lett.* **90**(6), 062908 (2007).
- [5] S. Q. Fang, Y. J. Qiao, X. H. Zhang, F. R. Ling, *Phys. Status Solidi A* **204**(3), 833 (2007).
- [6] D. McMillen, T. Hudson, J. Wagner, J. Singleton, *Opt. Express* **2**(12), 491 (1998).
- [7] Y. Liao, Y. B. Guo, L. C. Cao, X. S. Ma, Q. S. He, G. F. Jin, *Opt. Express* **12**(17), 4047 (2004).
- [8] Y. P. Yang, K. Buse, D. Psaltis, *Opt. Lett.* **27**(3), 158 (2002).
- [9] J. Imbrock, A. Wirp, D. Kip, E. Kräzig, *J. Opt. Soc. Am. B* **19**, 1822 (2002).
- [10] G. G. Zhong, J. Jian, Z. K. Wu, *Proceeding of the*

11-th International Conference on Quantum Electronics, New York, IEEE, 1980, p. 631.

[11] T. R. Volk, V. I. Pryalkin, N. M. Rubinina, *Opt. Lett.* **15**, 996 (1990).

[12] J. K. Yamanoto, K. Kitamura, N. Iyi, S. Kimura, Y. Furukawa, M. Sato, *Appl. Phys. Lett.* **61**, 2156 (1992).

[13] T. Volk, N. Rubinina, M. Wohlecke, *J. Opt. Soc. Am. B* **11**(9), 1681 (1994).

[14] T. Zhang, B. Wang, S. Q. Fang, Y. Q. Zhao, F. R. Ling, W. S. Xu, *Optik* **115**(5), 197 (2004).

[15] Y. H. Xu, W. S. Xu, S. W. Xu, B. Wang, *Opt. Mater.* **23**(1-2), 305 (2003).

[16] K. Buse, A. Adibi, and D. Psaltis, *Nature* **393**, 665 (1998).

[17] Y. Liu, L. Liu, C. Zhou, and L. Xu, *Opt. Lett.* **25**, 908 (2000).

[18] Y. Liu, L. Liu, D. Liu, L. Xu, and C. Zhou, *Opt. Commun.* **190**, 339 (2001).

[19] H. Kogelnik, *Bell Syst. Tech. J.* **48**, 2909 (1969).

[20] T. Zhang, T. Geng, W. M. Sun, D. C. Ma, F. R. Ling, *Mater. Chem. Phys.* **103**(1), 137 (2007).

[21] D. L. Staebler, J. J. Amodei, *J. Appl. Phys.* **43**, 1042 (1972).

[22] Z. Q. Jiang, X. Li, Y. B. Sun, S. Q. Tao, *Proc. of SPIE* **6827**, 68270W-1 (2007).

[23] W. Zhen, N. D. Zhang, L. C. Zhao, Y. H. Xu, *Opt. Commun.* **227**, 259 (2003).

[24] G. P. Nordin, P. Asthana, *Opt. Lett.* **18**(18), 1553 (1993).

\*Corresponding author. [tzhang\\_hit02@yahoo.com](mailto:tzhang_hit02@yahoo.com)